Short-range correlation physics at low RG resolution

Anthony Tropiano[1], Dick Furnstahl[1], Scott Bogner[2]

[1]Ohio State University, [2]Michigan State University

APS April Meeting – Virtual Meeting

April 19, 2021

ajt, S.K. Bogner, and R.J. Furnstahl, arXiv:2006.11186

*Phys. Rev. C **102**, 034005 (2020)*

ajt, S.K. Bogner, and R.J. Furnstahl, in progress

NUCLEI
Nuclear Computational Low-Energy Initiative

THE OHIO STATE UNIVERSITY

NSF

U.S. DEPARTMENT OF ENERGY

Motivation

- Recent experiments have been able to isolate processes where short-range correlation (SRC) physics is dominant and well accounted for by SRC phenomenology
- SRC physics at high RG resolution
    - SRC pairs are components in the nuclear wave function with relative momenta above the Fermi momentum

knock-out 2 high-k nucleons

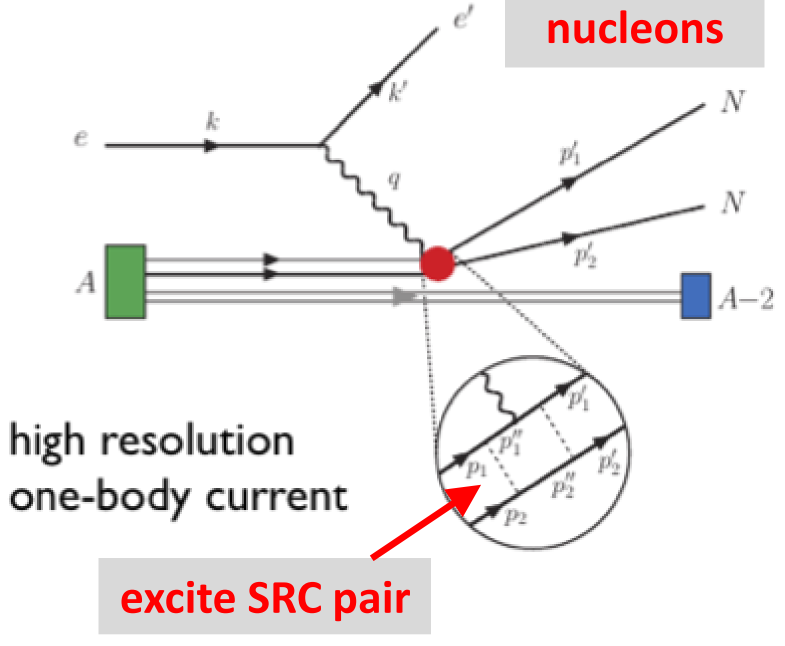

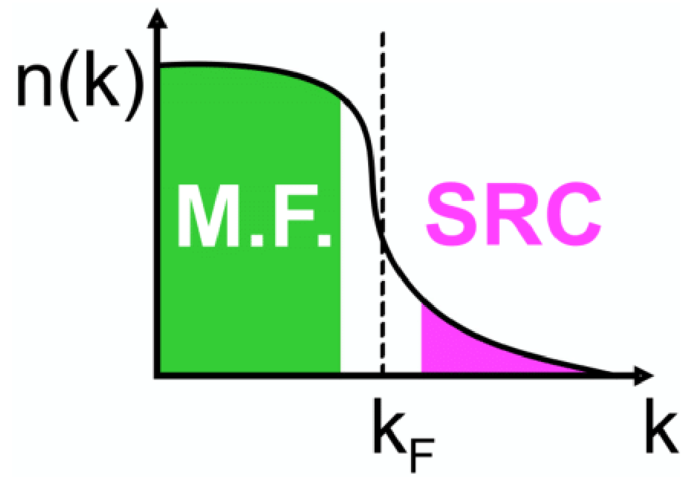

Motivation

- Recent experiments have been able to isolate processes where short-range correlation (SRC) physics is dominant and well accounted for by SRC phenomenology
- SRC physics at low RG resolution
  - The SRC *physics* is shifted into the reaction operators from the nuclear wave function (which becomes soft)
  - Operators do not become hard which simplifies calculations

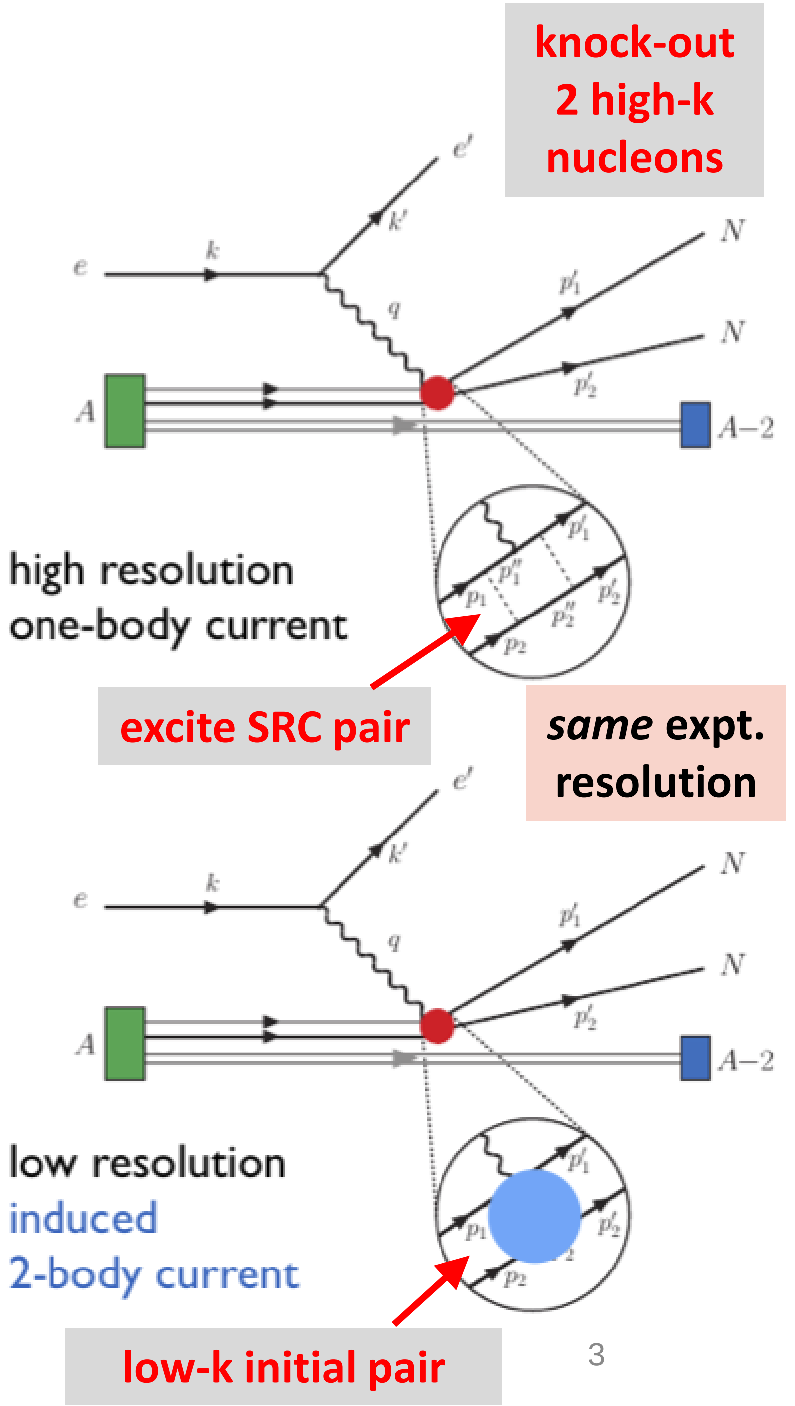

Motivation

- Recent experiments have been able to isolate processes where short-range correlation (SRC) physics is dominant and well accounted for by SRC phenomenology
- SRC physics at low RG resolution
  - The SRC *physics* is shifted into the reaction operators from the nuclear wave function (which becomes soft)
  - Operators do not become hard which simplifies calculations
- Experimental resolution (set by momentum of probe) is the same in both pictures
- Same observables but different physical interpretation!

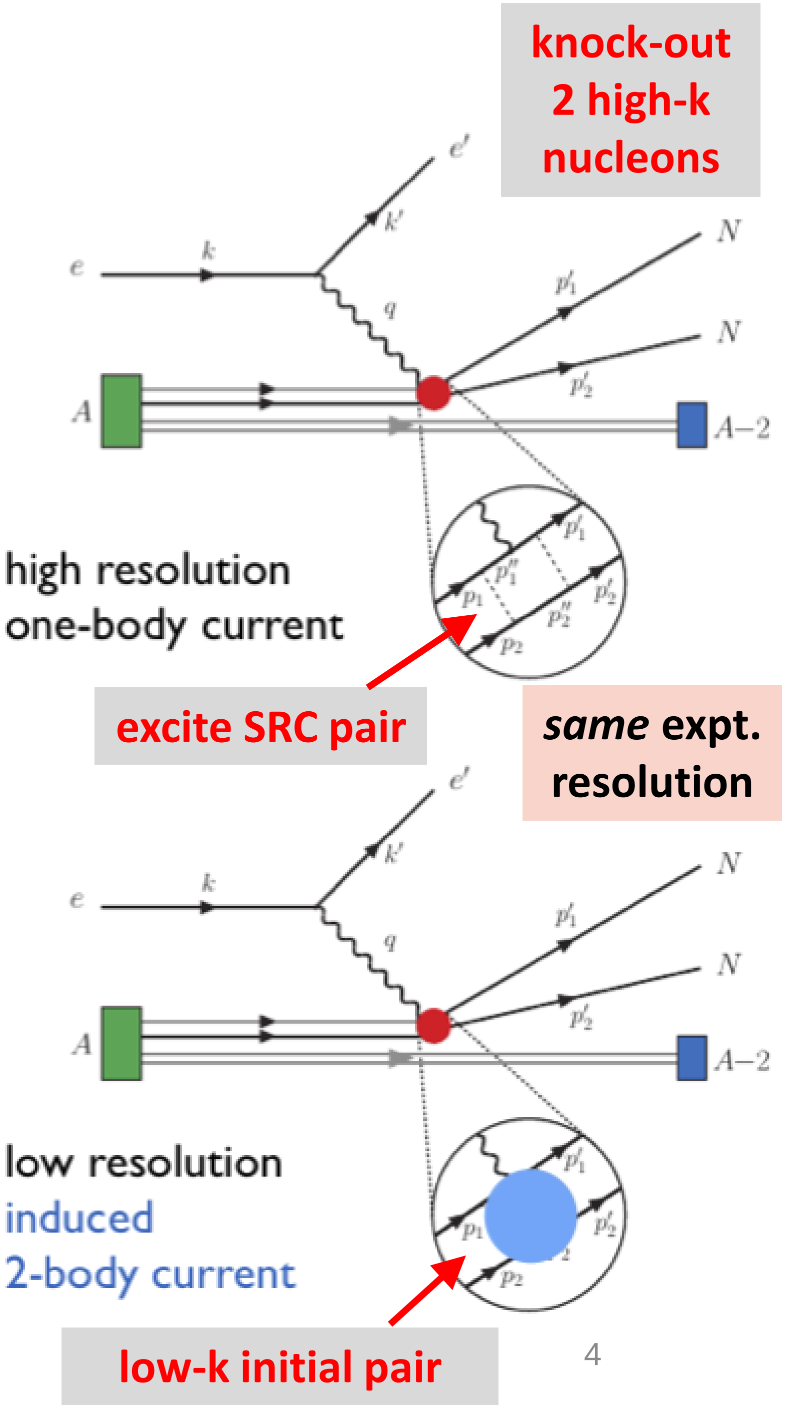

Similarity Renormalization Group (SRG)

- Evolve operators to low RG resolution

$$O(s) = U(s)O(0)U^{\dagger}(s)$$

where $s = 0 \rightarrow \infty$ and $U(s)$ is unitary

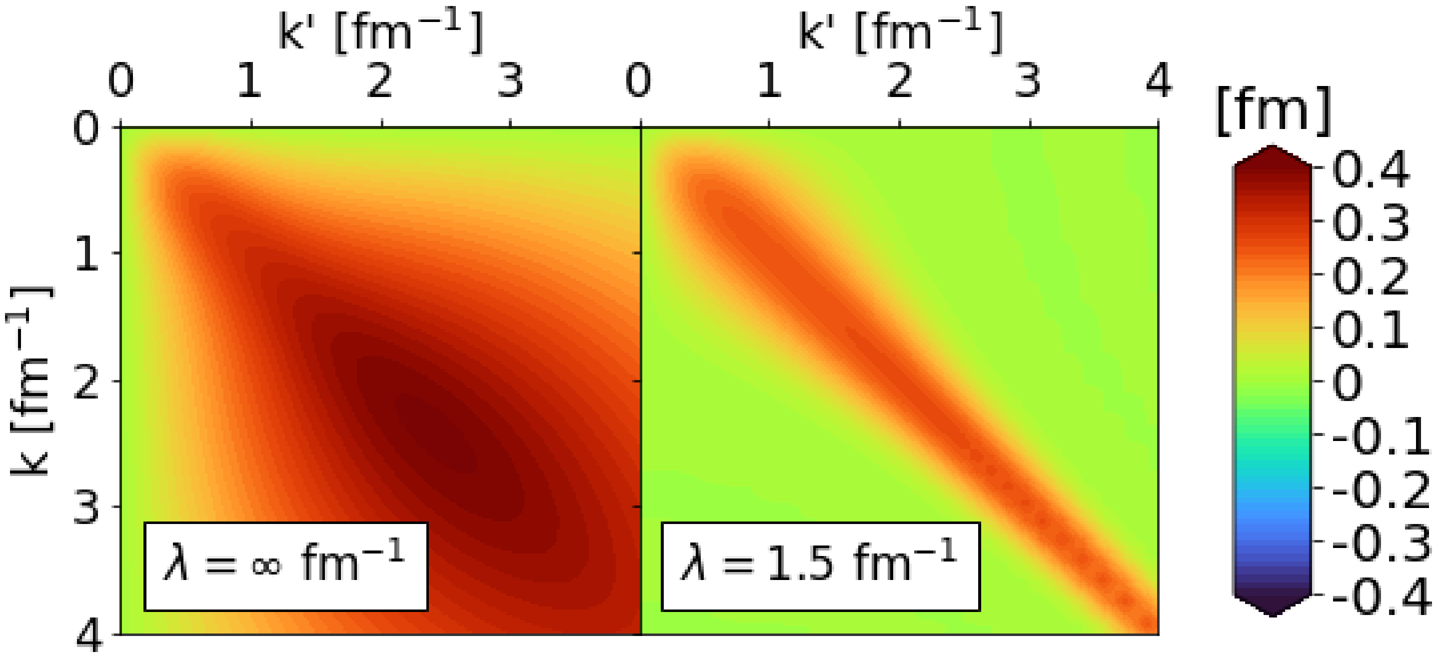

Fig. 1: Momentum space matrix elements of Argonne v18 (AV18) under SRG evolution in $^1P_1$ channel.

Similarity Renormalization Group (SRG)

- Evolve operators to low RG resolution

  $$O(s) = U(s)O(0)U^{\dagger}(s)$$

  where $s = 0 \rightarrow \infty$ and $U(s)$ is unitary
- $\lambda = s^{-1/4}$ describes the decoupling scale of the RG evolved operator

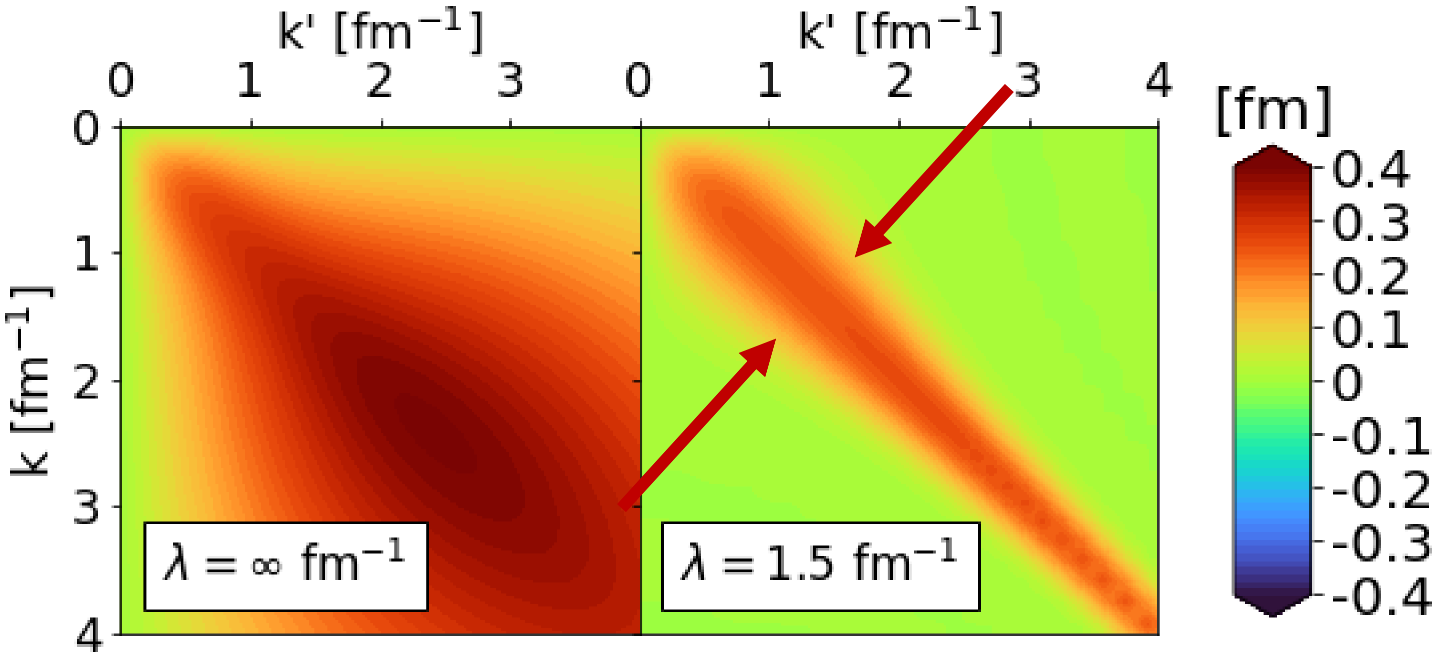

Fig. 1: Momentum space matrix elements of Argonne v18 (AV18) under SRG evolution in $^1P_1$ channel.

Deuteron wave function at low RG resolution

- AV18 wave function has significant SRC
- What happens to the wave function at low RG resolution?

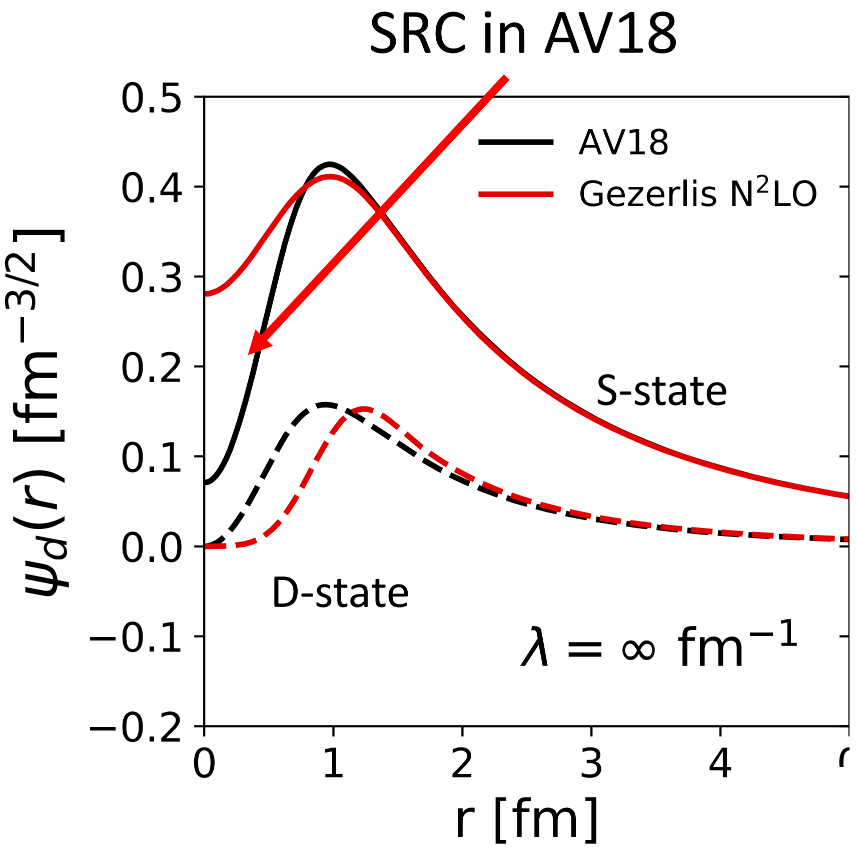

Fig. 2: SRG evolution of deuteron wave function in coordinate space for AV18 and Gezerlis N2LO[1].

[1]A. Gezerlis et al., Phys. Rev. C **90**, 054323 (2014)

Deuteron wave function at low RG resolution

- SRC physics in AV18 is gone from wave function at low RG resolution
- Deuteron wave functions become soft and D-state probability goes down
- Observables such as asymptotic D-S ratio are the same

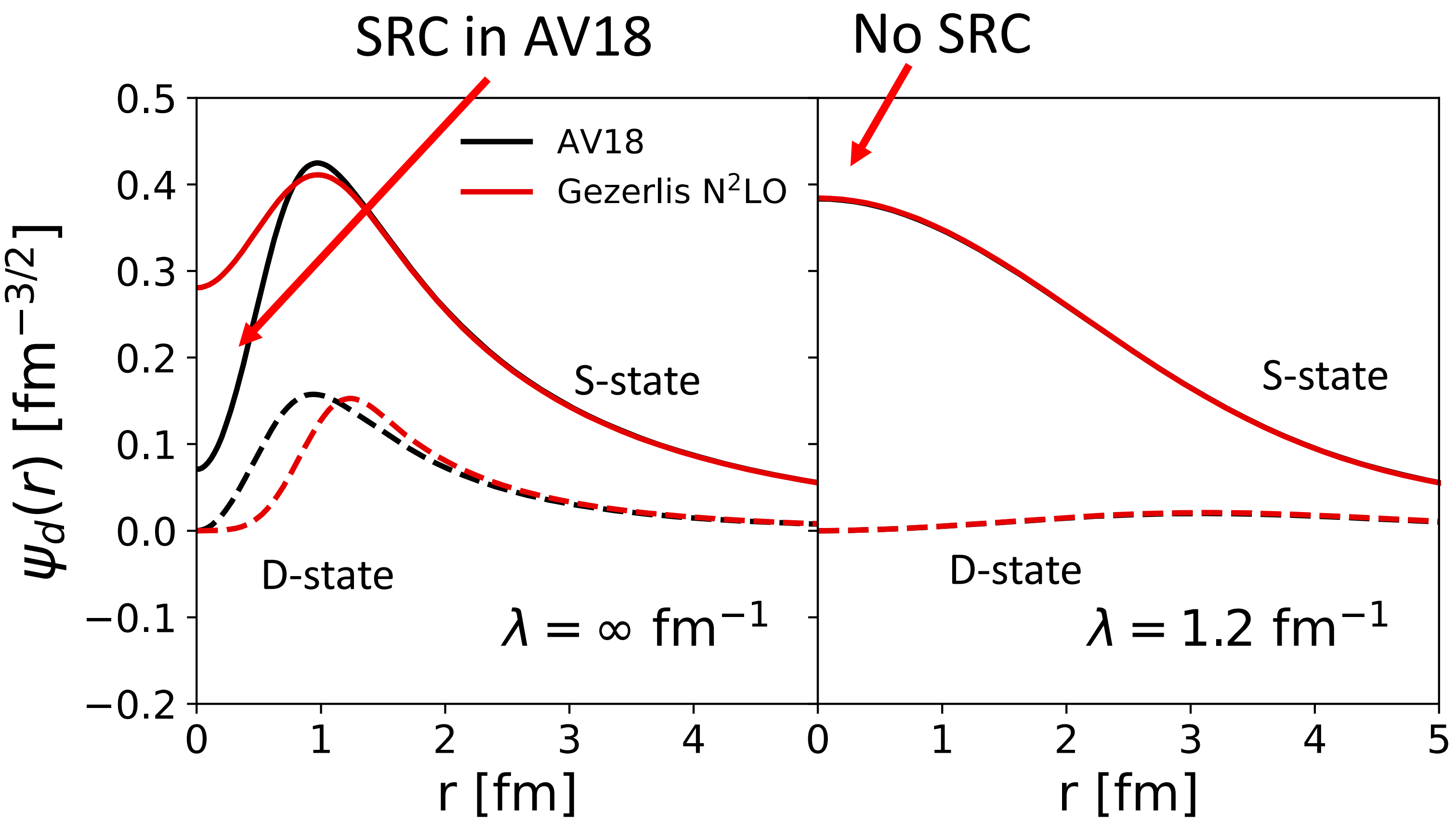

Fig. 2: SRG evolution of deuteron wave function in coordinate space for AV18 and Gezerlis N2LO[1].

[1]A. Gezerlis et al., Phys. Rev. C **90**, 054323 (2014)

Momentum distributions at low RG resolution

- Soft wave functions at low RG resolution
  - Where does the SRC physics go?

Momentum distributions at low RG resolution

- Soft wave functions at low RG resolution
  - Where does the SRC physics go?
- SRC physics shifts to the operators $\langle\psi_f^{hi}|U_\lambda^\dagger U_\lambda O^{hi} U_\lambda^\dagger U_\lambda|\psi_i^{hi}\rangle$
- Apply SRG transformations to momentum distribution operator

$$n^{hi}(\boldsymbol{q}) = a_{\boldsymbol{q}}^\dagger a_{\boldsymbol{q}}$$

$$U_\lambda = 1 + \frac{1}{4}\sum_{\boldsymbol{K},\boldsymbol{k},\boldsymbol{k}'} \delta U_\lambda^{(2)}(\boldsymbol{k},\boldsymbol{k}') a_{\frac{\boldsymbol{K}}{2}+\boldsymbol{k}}^\dagger a_{\frac{\boldsymbol{K}}{2}-\boldsymbol{k}}^\dagger a_{\frac{\boldsymbol{K}}{2}-\boldsymbol{k}'} a_{\frac{\boldsymbol{K}}{2}+\boldsymbol{k}'} + \cdots$$

Momentum distributions at low RG resolution

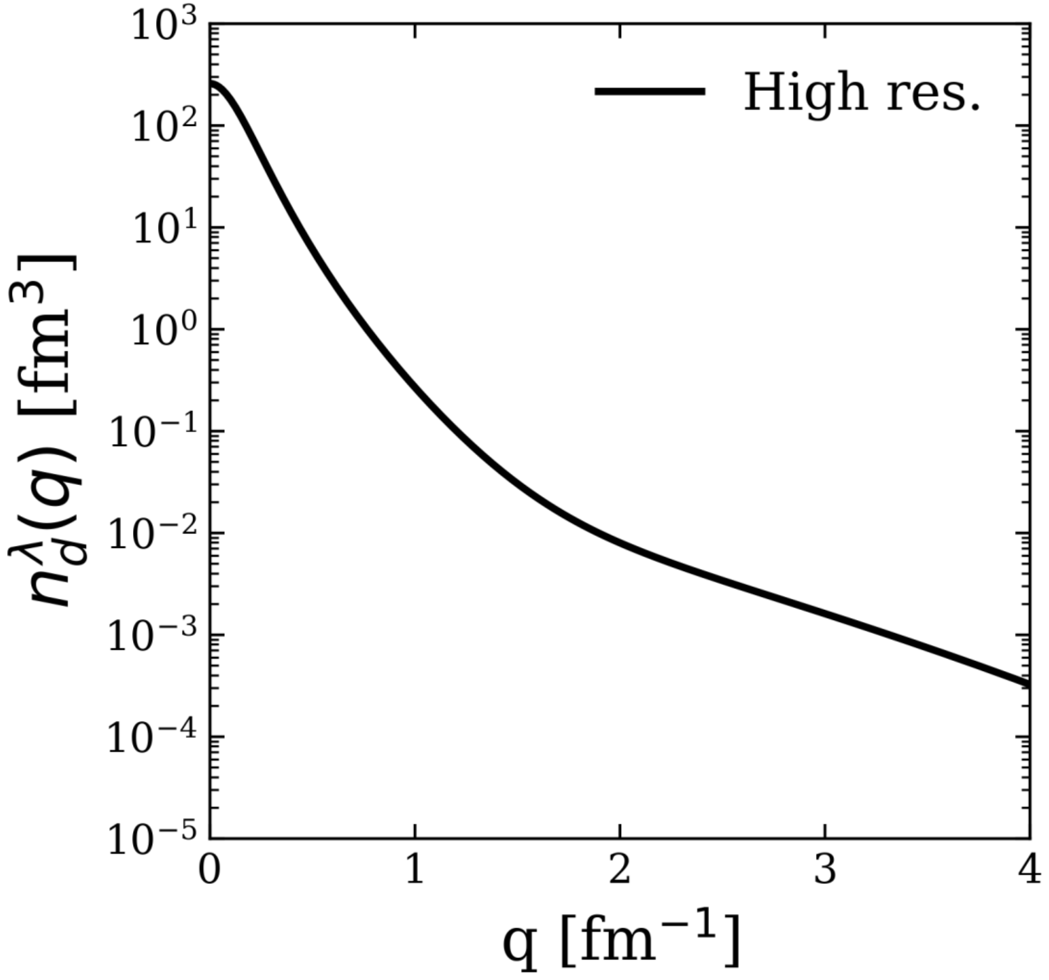

Fig. 3: Contributions to deuteron momentum distribution with AV18 and $\lambda = 1.35$ fm^{-1}.

- Deuteron example

$$n^{lo}(\boldsymbol{q}) = (1 + \delta U) a_{\boldsymbol{q}}^\dagger a_{\boldsymbol{q}} (1 + \delta U^\dagger)$$

$$\langle \psi_d^{hi} | a_{\boldsymbol{q}}^\dagger a_{\boldsymbol{q}} | \psi_d^{hi} \rangle$$

Momentum distributions at low RG resolution

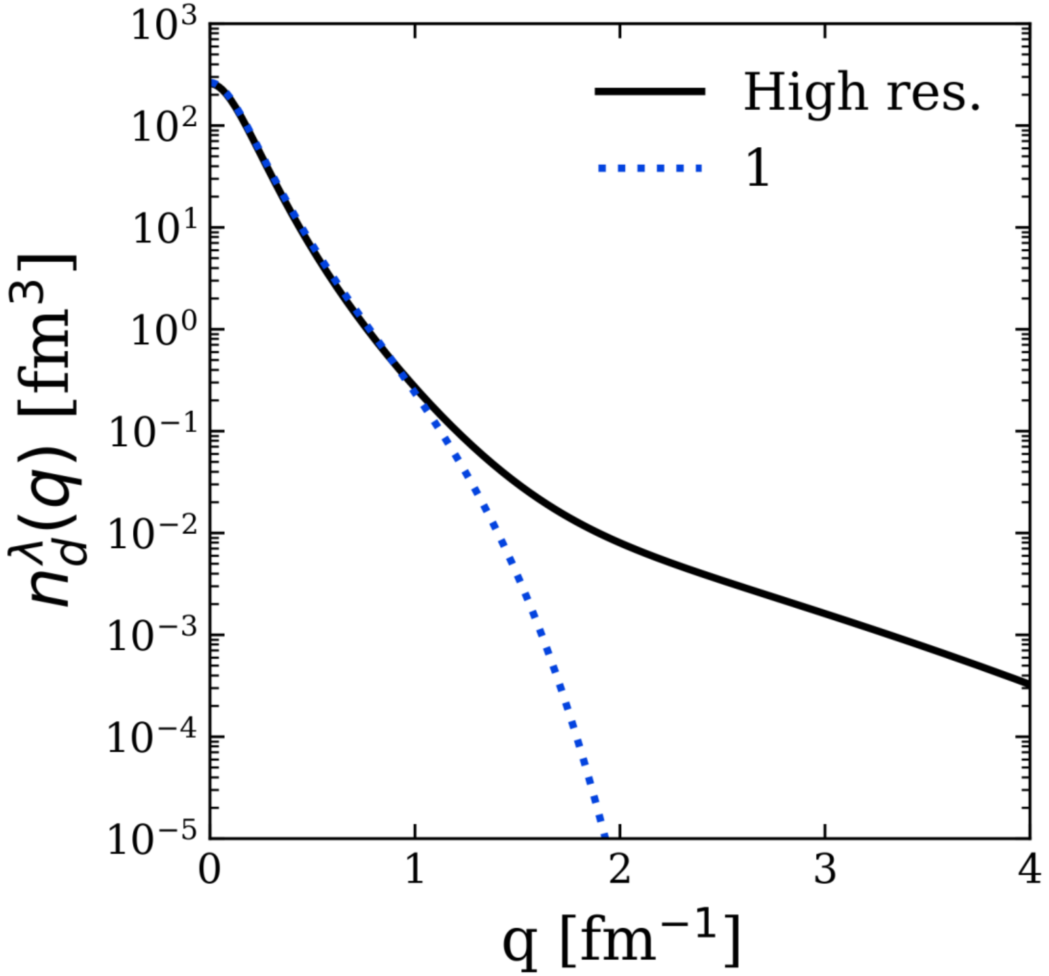

Fig. 3: Contributions to deuteron momentum distribution with AV18 and $\lambda = 1.35$ fm^{-1}.

- Deuteron example

$$n^{lo}(\boldsymbol{q}) = (1 + \delta U) a_{\boldsymbol{q}}^\dagger a_{\boldsymbol{q}} (1 + \delta U^\dagger)$$

$$\langle \psi_d^{hi} | a_{\boldsymbol{q}}^\dagger a_{\boldsymbol{q}} | \psi_d^{hi} \rangle$$

$$\langle \psi_d^{lo} | a_{\boldsymbol{q}}^\dagger a_{\boldsymbol{q}} | \psi_d^{lo} \rangle$$

Momentum distributions at low RG resolution

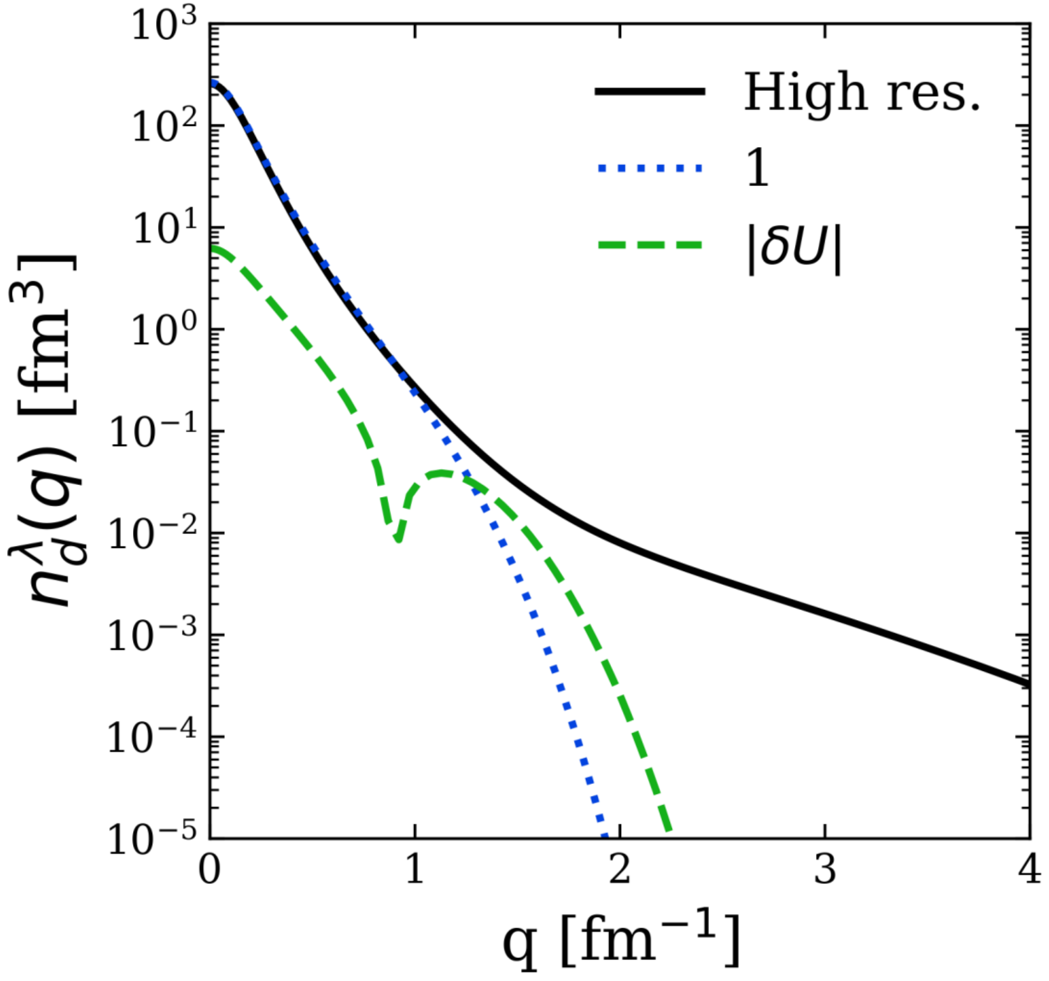

Fig. 3: Contributions to deuteron momentum distribution with AV18 and $\lambda = 1.35$ fm^{-1}.

- Deuteron example

$$n^{lo}(\boldsymbol{q}) = (1 + \delta U) a_{\boldsymbol{q}}^\dagger a_{\boldsymbol{q}} (1 + \delta U^\dagger)$$

$$\langle \psi_d^{hi} | a_{\boldsymbol{q}}^\dagger a_{\boldsymbol{q}} | \psi_d^{hi} \rangle$$

$$\langle \psi_d^{lo} | a_{\boldsymbol{q}}^\dagger a_{\boldsymbol{q}} | \psi_d^{lo} \rangle$$

$$\langle \psi_d^{lo} | \delta U a_{\boldsymbol{q}}^\dagger a_{\boldsymbol{q}} + a_{\boldsymbol{q}}^\dagger a_{\boldsymbol{q}} \delta U^\dagger | \psi_d^{lo} \rangle$$

Momentum distributions at low RG resolution

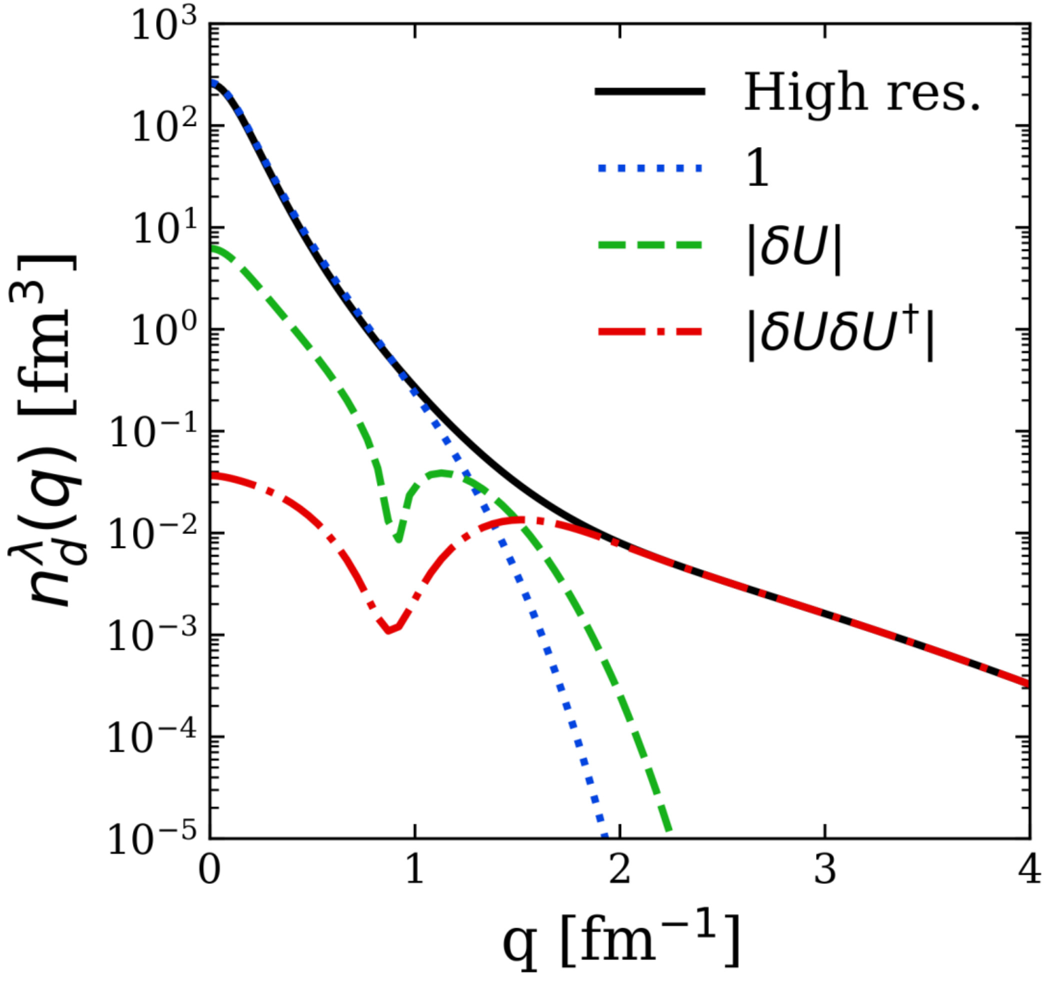

Fig. 3: Contributions to deuteron momentum distribution with AV18 and $\lambda = 1.35$ fm^{-1}.

- Deuteron example

$$n^{lo}(\boldsymbol{q}) = (1 + \delta U) a_{\boldsymbol{q}}^\dagger a_{\boldsymbol{q}} (1 + \delta U^\dagger)$$

$$\langle \psi_d^{hi} | a_{\boldsymbol{q}}^\dagger a_{\boldsymbol{q}} | \psi_d^{hi} \rangle$$

$$\langle \psi_d^{lo} | a_{\boldsymbol{q}}^\dagger a_{\boldsymbol{q}} | \psi_d^{lo} \rangle$$

$$\langle \psi_d^{lo} | \delta U a_{\boldsymbol{q}}^\dagger a_{\boldsymbol{q}} + a_{\boldsymbol{q}}^\dagger a_{\boldsymbol{q}} \delta U^\dagger | \psi_d^{lo} \rangle$$

$$\langle \psi_d^{lo} | \delta U a_{\boldsymbol{q}}^\dagger a_{\boldsymbol{q}} \delta U^\dagger | \psi_d^{lo} \rangle$$

Momentum distributions at low RG resolution

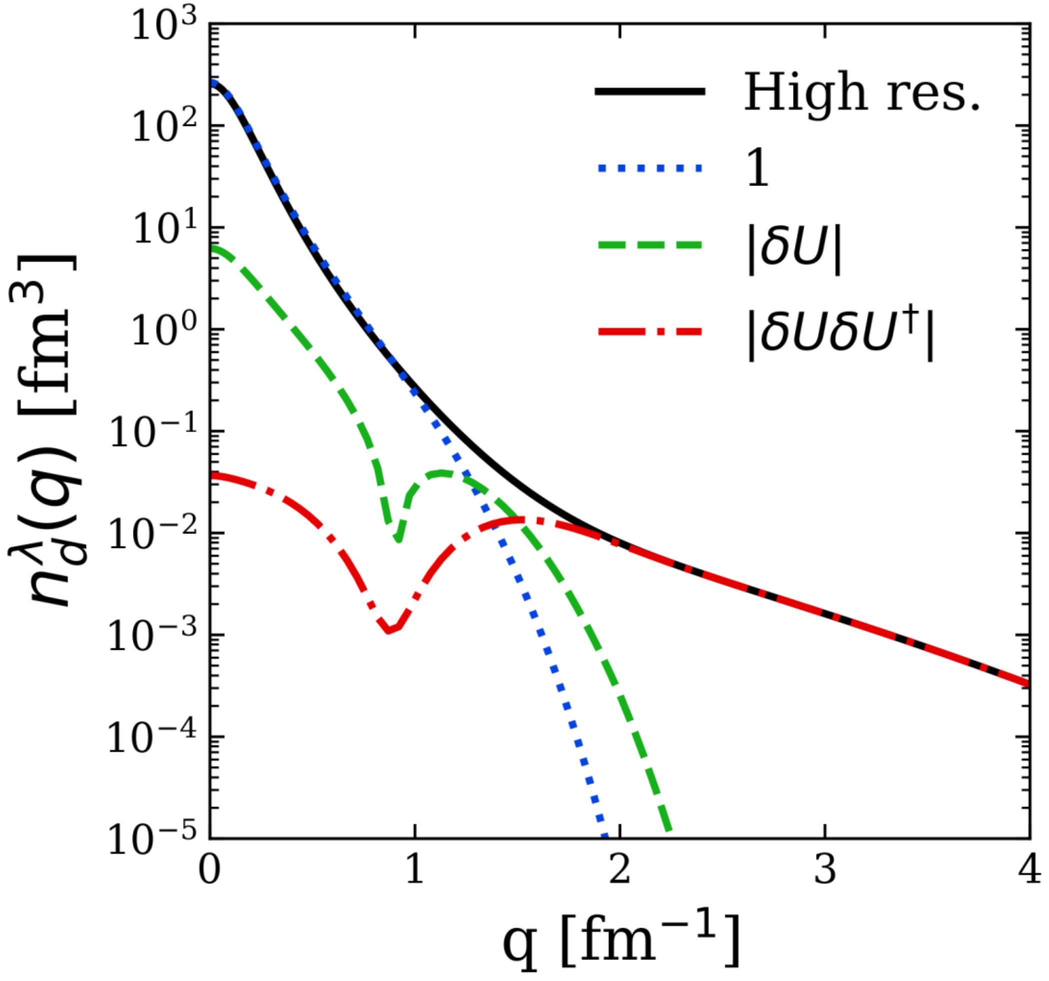

Fig. 3: Contributions to deuteron momentum distribution with AV18 and $\lambda = 1.35$ fm^{-1}.

- For high-q, the $\delta U_\lambda \delta U_\lambda^\dagger$ 2-body term dominates

$$\approx \sum_{\boldsymbol{K},\boldsymbol{k},\boldsymbol{k}'} \delta U_\lambda(\boldsymbol{k},\boldsymbol{q}) \delta U_\lambda^\dagger(\boldsymbol{q},\boldsymbol{k}') a^\dagger_{\frac{\boldsymbol{K}}{2}+\boldsymbol{k}} a^\dagger_{\frac{\boldsymbol{K}}{2}-\boldsymbol{k}} a_{\frac{\boldsymbol{K}}{2}-\boldsymbol{k}'} a_{\frac{\boldsymbol{K}}{2}+\boldsymbol{k}'}$$

Momentum distributions at low RG resolution

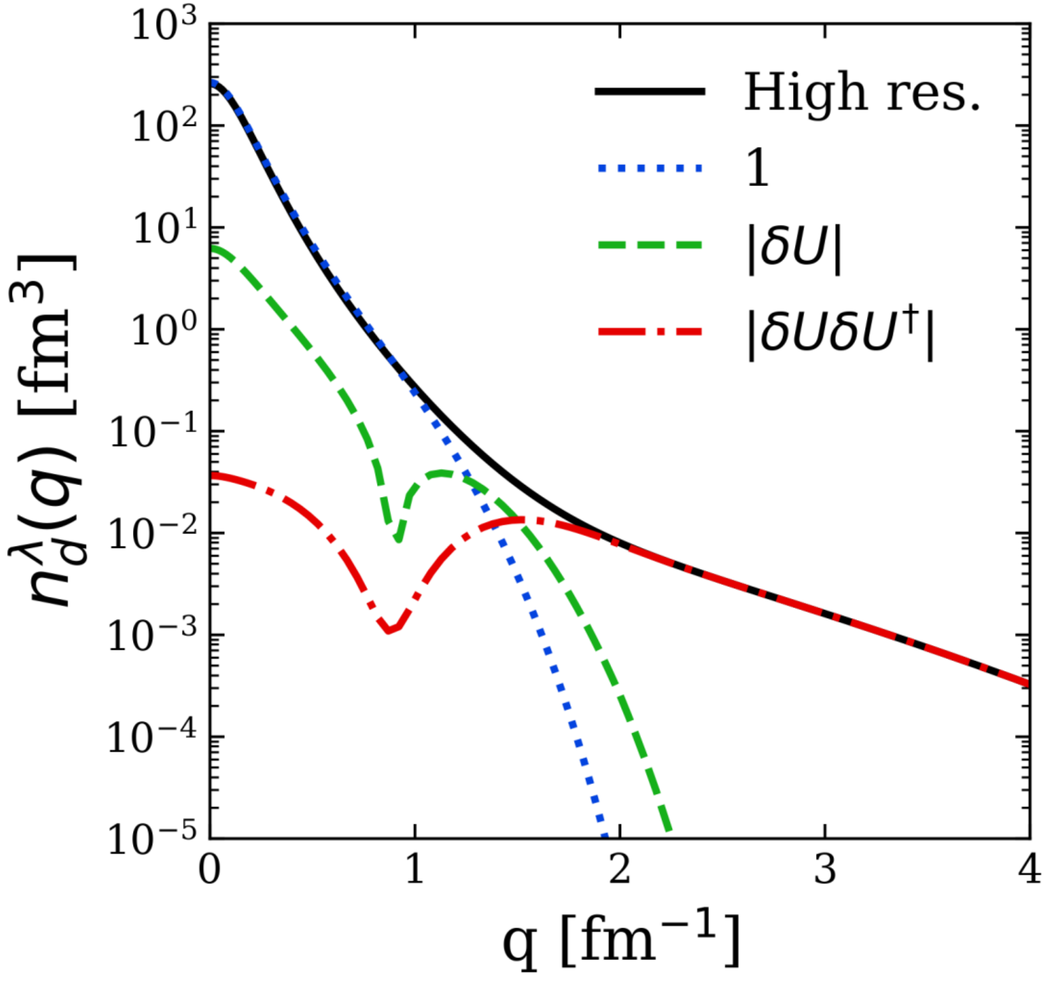

Fig. 3: Contributions to deuteron momentum distribution with AV18 and $\lambda = 1.35$ fm^{-1}.

- For high-q, the $\delta U_\lambda \delta U_\lambda^\dagger$ 2-body term dominates

$$\approx \sum_{\boldsymbol{K},\boldsymbol{k},\boldsymbol{k}'} \delta U_\lambda(\boldsymbol{k},\boldsymbol{q}) \delta U_\lambda^\dagger(\boldsymbol{q},\boldsymbol{k}') a^\dagger_{\frac{\boldsymbol{K}}{2}+\boldsymbol{k}} a^\dagger_{\frac{\boldsymbol{K}}{2}-\boldsymbol{k}} a_{\frac{\boldsymbol{K}}{2}-\boldsymbol{k}'} a_{\frac{\boldsymbol{K}}{2}+\boldsymbol{k}'}$$

$\downarrow$

Factorization: $\delta U_\lambda(\boldsymbol{k},\boldsymbol{q}) \approx F_\lambda^{lo}(\boldsymbol{k}) F_\lambda^{hi}(\boldsymbol{q})$

$\downarrow$

$$\approx \left| F_\lambda^{hi}(\boldsymbol{q}) \right|^2 \sum_{\boldsymbol{K},\boldsymbol{k},\boldsymbol{k}'}^{\lambda} F_\lambda^{lo}(\boldsymbol{k}) F_\lambda^{lo}(\boldsymbol{k}') a^\dagger_{\frac{\boldsymbol{K}}{2}+\boldsymbol{k}} a^\dagger_{\frac{\boldsymbol{K}}{2}-\boldsymbol{k}} a_{\frac{\boldsymbol{K}}{2}-\boldsymbol{k}'} a_{\frac{\boldsymbol{K}}{2}+\boldsymbol{k}'}$$

Momentum distributions at low RG resolution

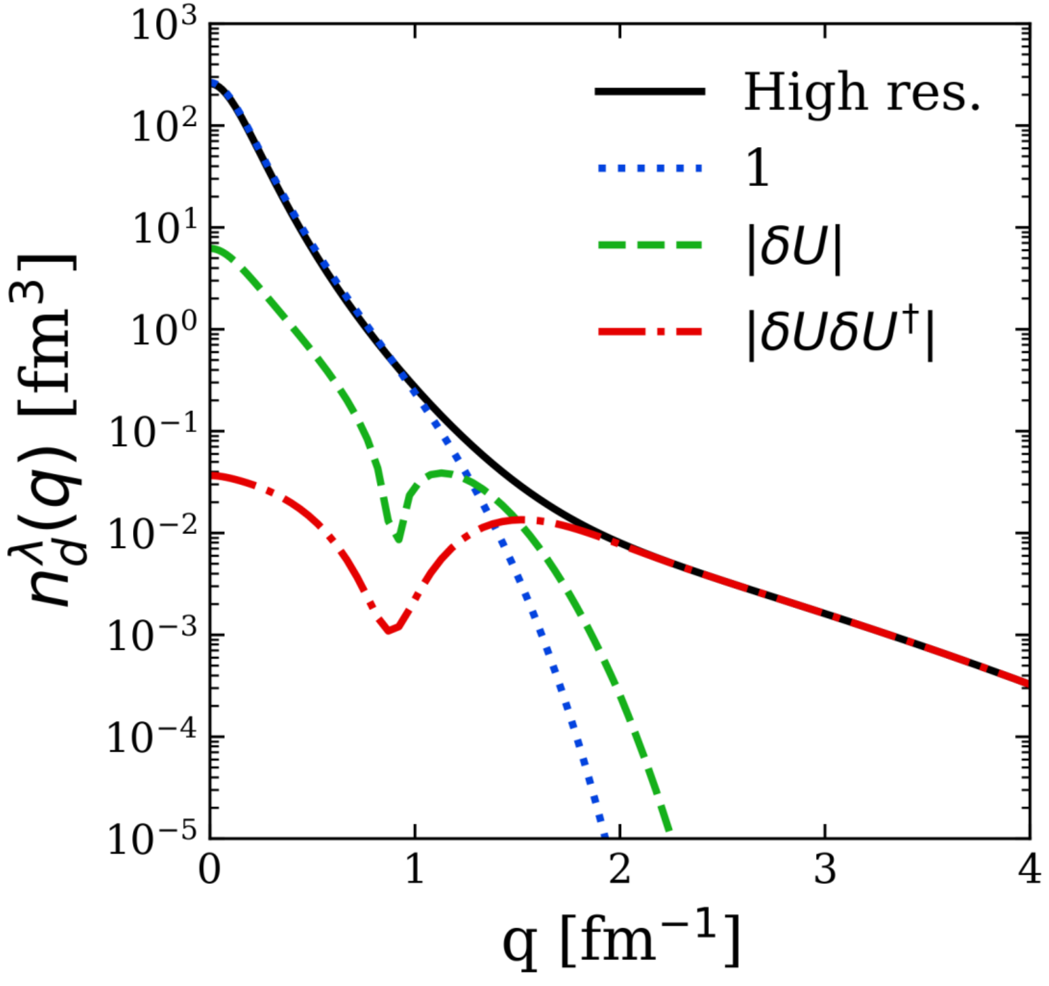

Fig. 3: Contributions to deuteron momentum distribution with AV18 and $\lambda = 1.35$ fm^{-1}.

- For high-q, the $\delta U_\lambda \delta U_\lambda^\dagger$ 2-body term dominates

$$\approx \sum \delta U_\lambda(\boldsymbol{k},\boldsymbol{q}) \delta U_\lambda^\dagger(\boldsymbol{q},\boldsymbol{k}') a^\dagger_{\frac{\boldsymbol{K}}{2}+\boldsymbol{k}} a^\dagger_{\frac{\boldsymbol{K}}{2}-\boldsymbol{k}} a_{\frac{\boldsymbol{K}}{2}-\boldsymbol{k}'} a_{\frac{\boldsymbol{K}}{2}+\boldsymbol{k}'}$$

Apply this strategy to nuclear momentum distributions using local density approximation (LDA)!

$F_\lambda^{hi}(\boldsymbol{q})$

$$\approx \left|F_\lambda^{lo}(\boldsymbol{q})\right|^2 \sum_{\boldsymbol{K},\boldsymbol{k},\boldsymbol{k}'} F_\lambda^{lo}(\boldsymbol{k}) F_\lambda^{lo}(\boldsymbol{k}') a^\dagger_{\frac{\boldsymbol{K}}{2}+\boldsymbol{k}} a^\dagger_{\frac{\boldsymbol{K}}{2}-\boldsymbol{k}} a_{\frac{\boldsymbol{K}}{2}-\boldsymbol{k}'} a_{\frac{\boldsymbol{K}}{2}+\boldsymbol{k}'}$$

Preliminary LDA results

- Universality
  - High-q tail collapses to universal function $\approx \left|F_{\lambda}^{hi}(\boldsymbol{q})\right|^2$ fixed by 2-body

Fig. 4: Proton momentum distribution under LDA with AV18 and $\lambda = 1.35$ fm^{-1}.

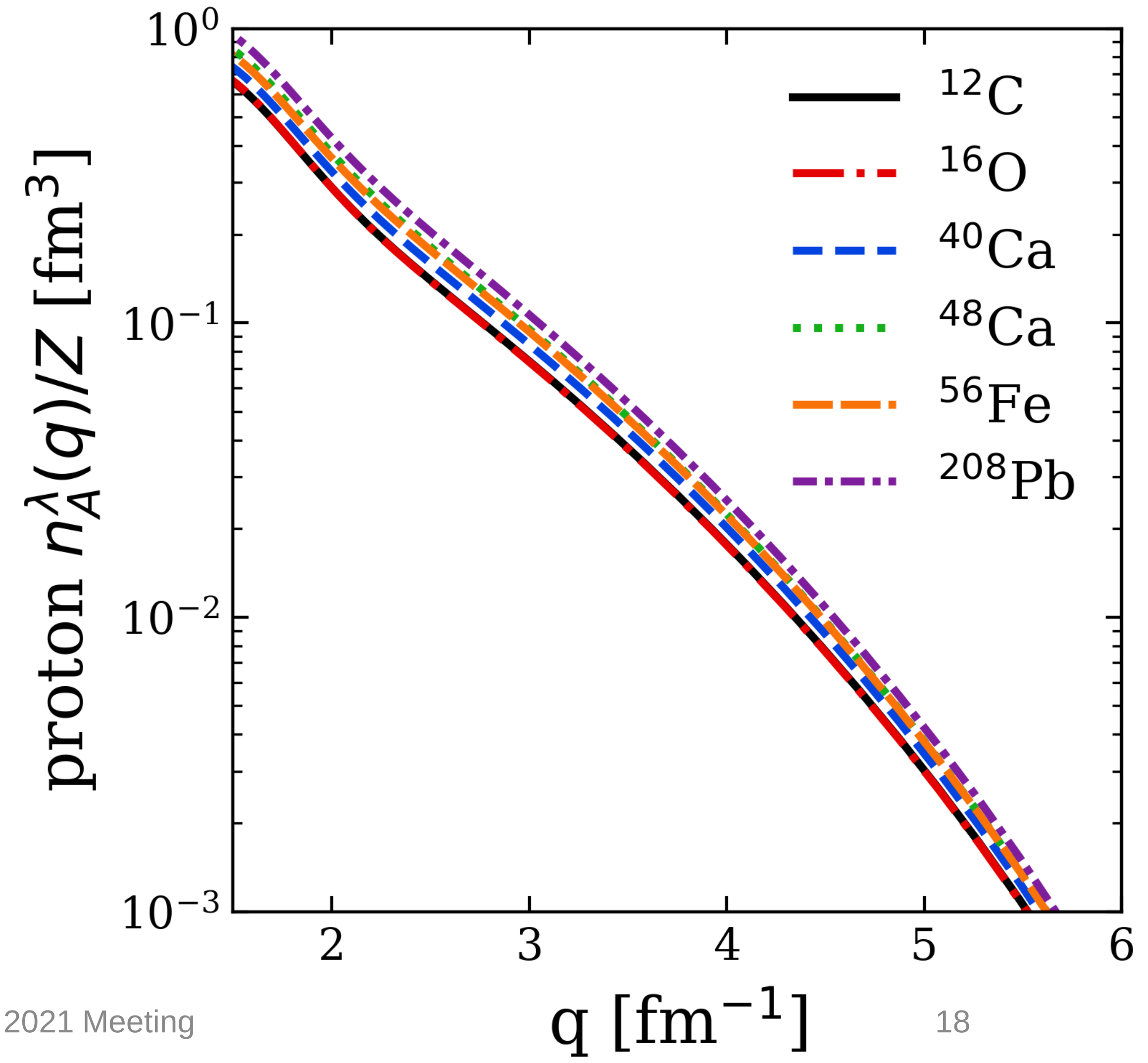

[1]R.B. Wiringa et al., Phys. Rev. C **89**, 024305 (2014)
https://www.phy.anl.gov/theory/research/momenta/

Preliminary LDA results

- Low RG resolution calculations reproduce momentum distributions of AV18 data[1] (high RG resolution calculation)
    - Low RG works well with simple approximations and is systematically improvable
    - *Absolute normalization still a work in progress (scaled up by one overall factor)*

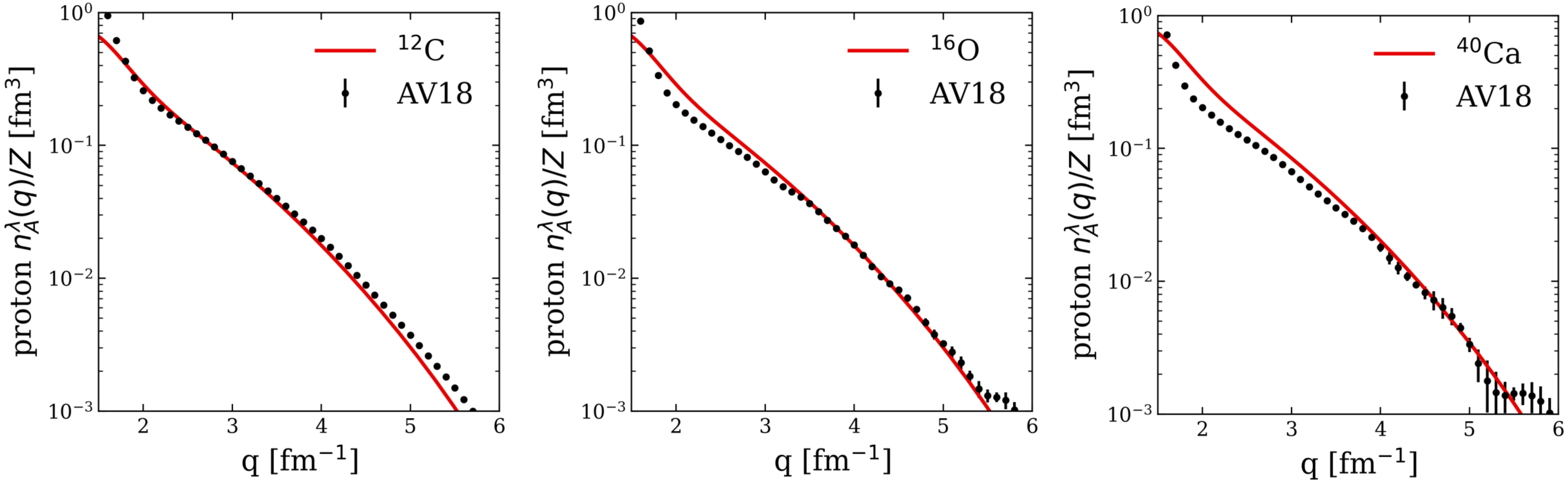

Fig. 5: Proton momentum distributions for ^{12}C, ^{16}O, and ^{40}Ca under LDA with AV18 and $\lambda = 1.35$ fm^{-1}.

Preliminary LDA results

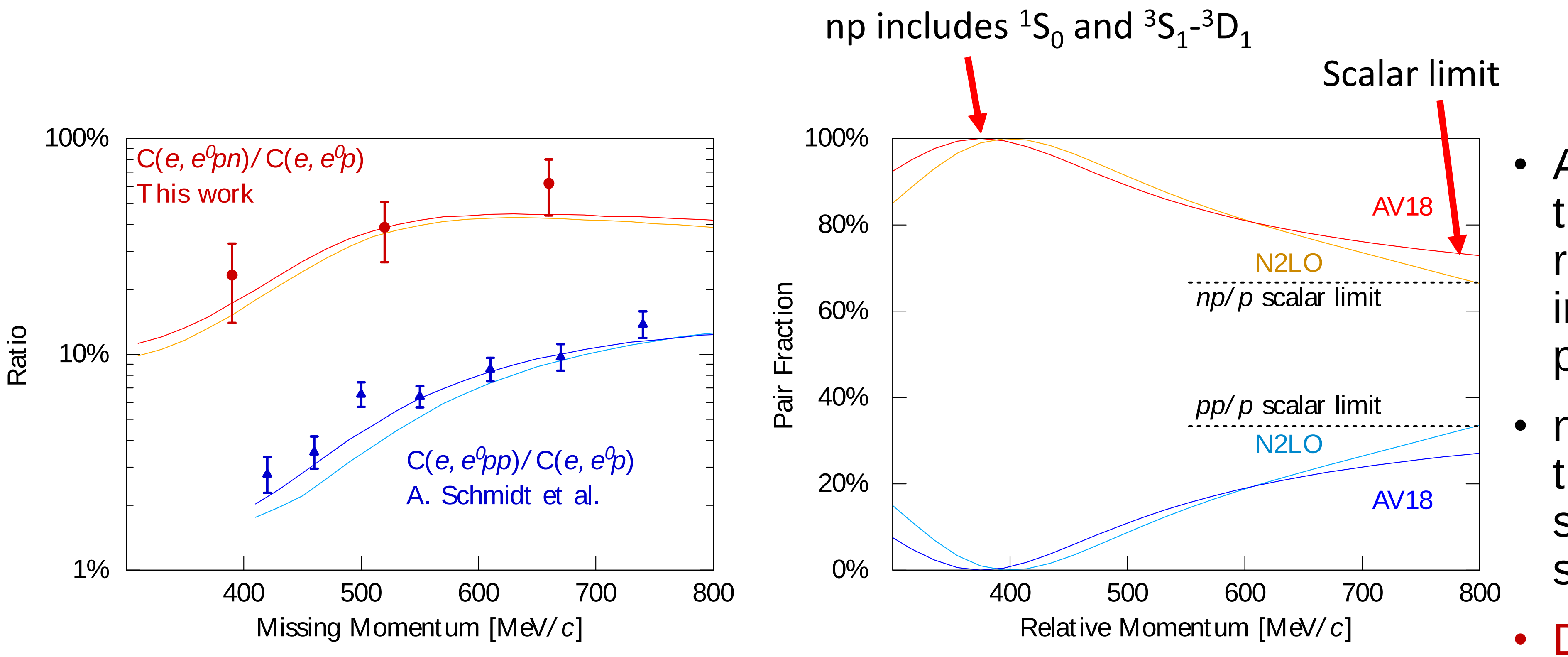

Fig. 6: (a) Ratio of two-nucleon to single-nucleon electron-scattering cross sections for carbon as a function of missing momentum. (b) Fraction of np to p and pp to p pairs versus the relative momentum. Figure from CLAS collaboration publication[1].

- At high RG resolution, the tensor force and the repulsive core of the NN interaction kicks nucleon pairs into SRCs
- np dominates because the tensor force requires spin triplet pairs (pp are spin singlets)
- Do we describe this physics at low RG resolution?

[1]I. Korover et al. (CLAS), arXiv:2004.07304 (2014)

Preliminary LDA results

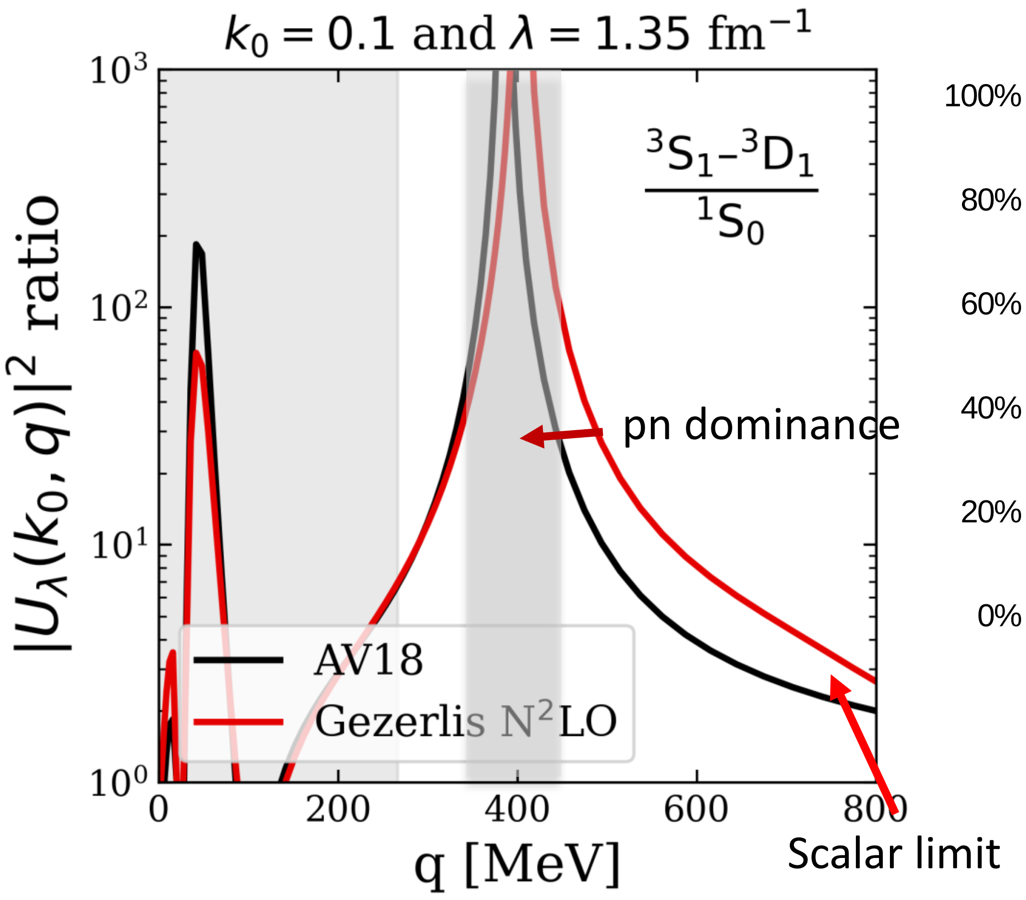

Fig. 7: $^3S_1$-$^3D_1$ to $^1S_0$ ratio of SRG-evolved momentum projection operators $a_q^\dagger a_q$.

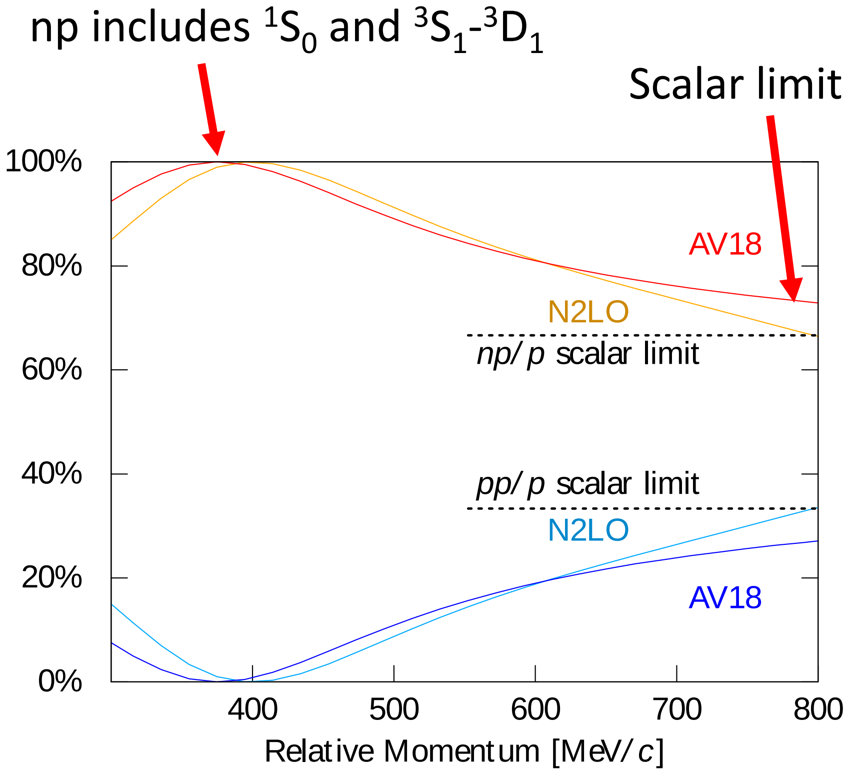

- At low RG resolution, SRCs are suppressed in the wave function
- Consider the ratio of $^3S_1$-$^3D_1$ to $^1S_0$ evolved momentum projection operator $a_q^\dagger a_q$
- This physics is established in the 2-body system!
- Can apply to any nucleus!

Preliminary LDA results

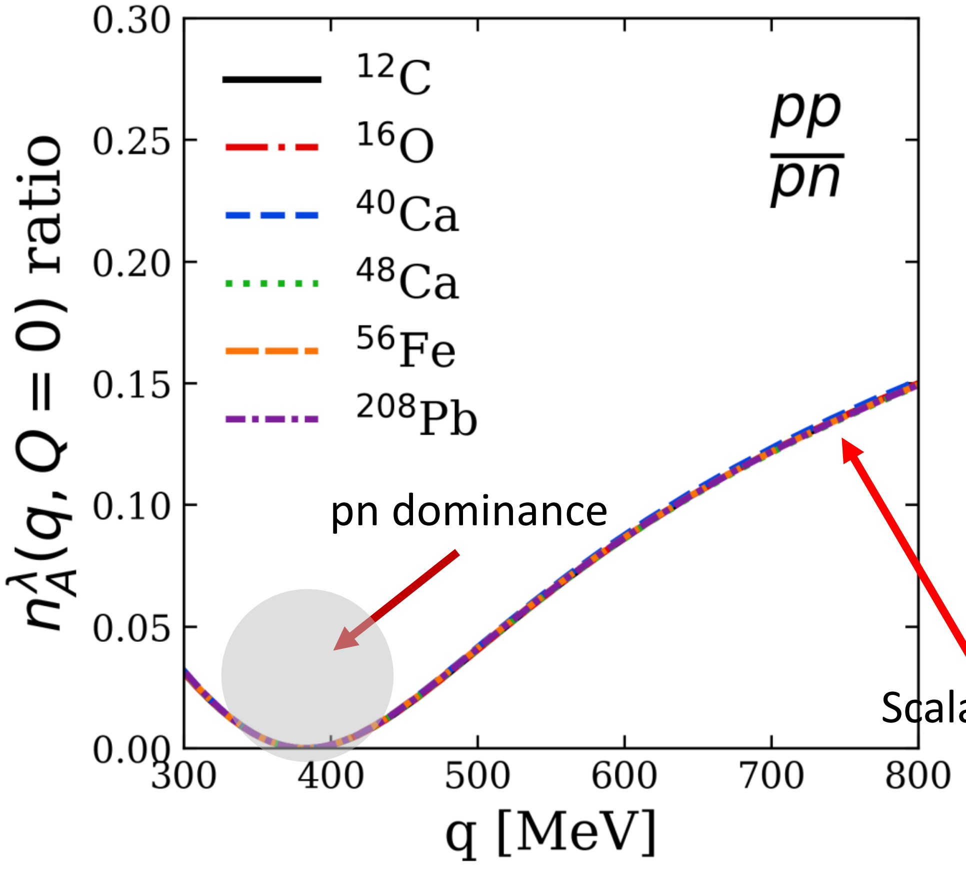

Fig. 8: pp/pn ratio of pair momentum distributions under LDA with AV18 and $\lambda = 1.35$ fm^{-1}.

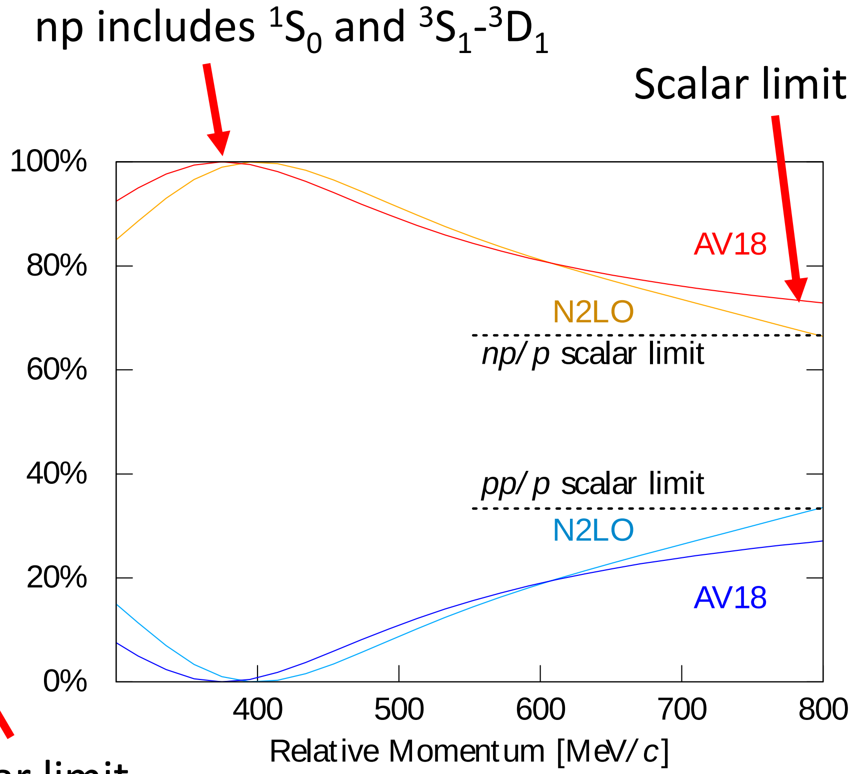

- Reproduces the characteristics of cross section ratios using low RG resolution operator with simple approximations

Preliminary LDA results

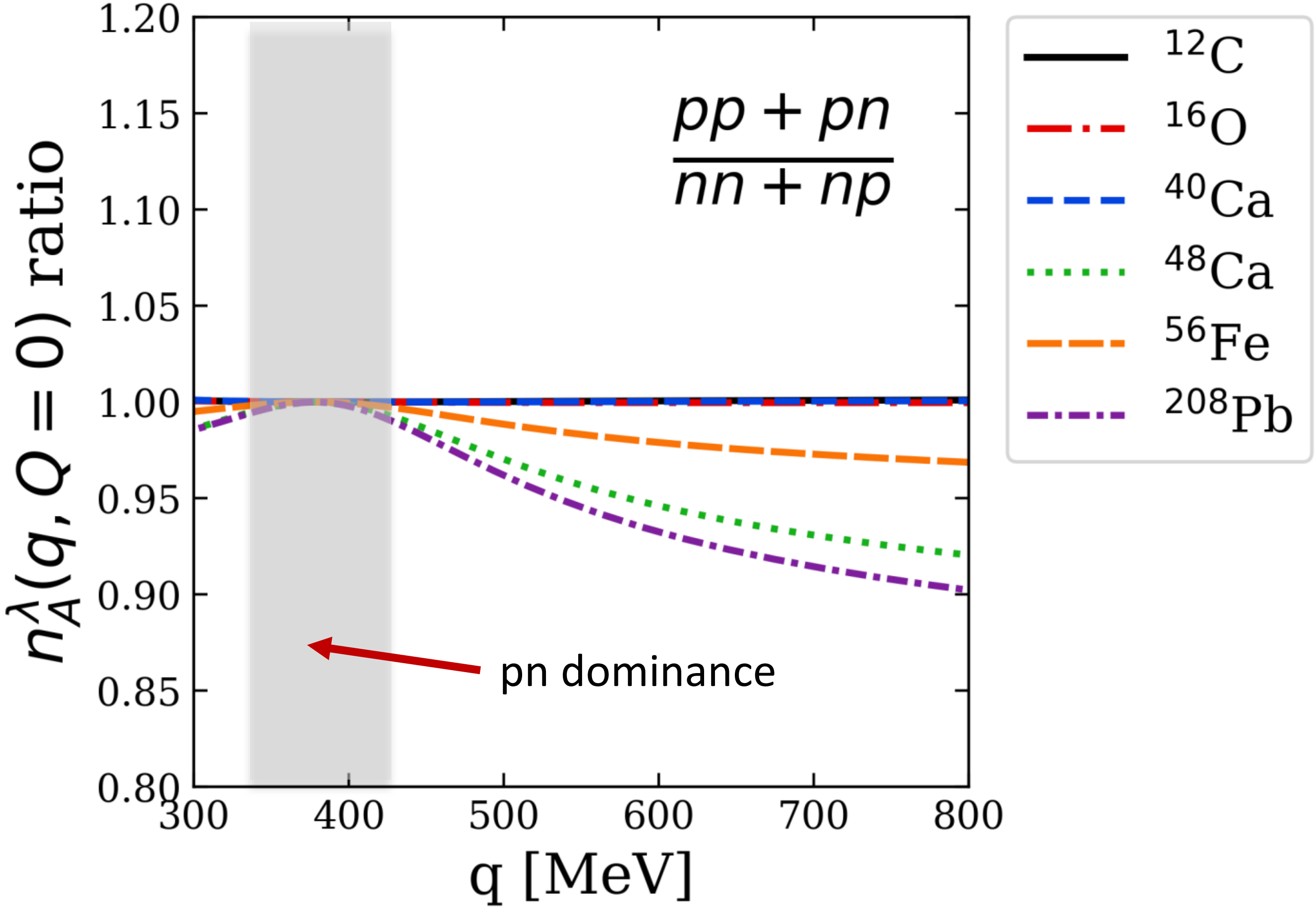

Fig. 9: (pp+pn)/(nn+np) ratio of pair momentum distributions under LDA with AV18 and $\lambda = 1.35$ fm^{-1}.

- Ratio ~1 independent of N/Z in pn dominant region
- Ratio < 1 for nuclei where N > Z and outside pn dominant region

Preliminary LDA results

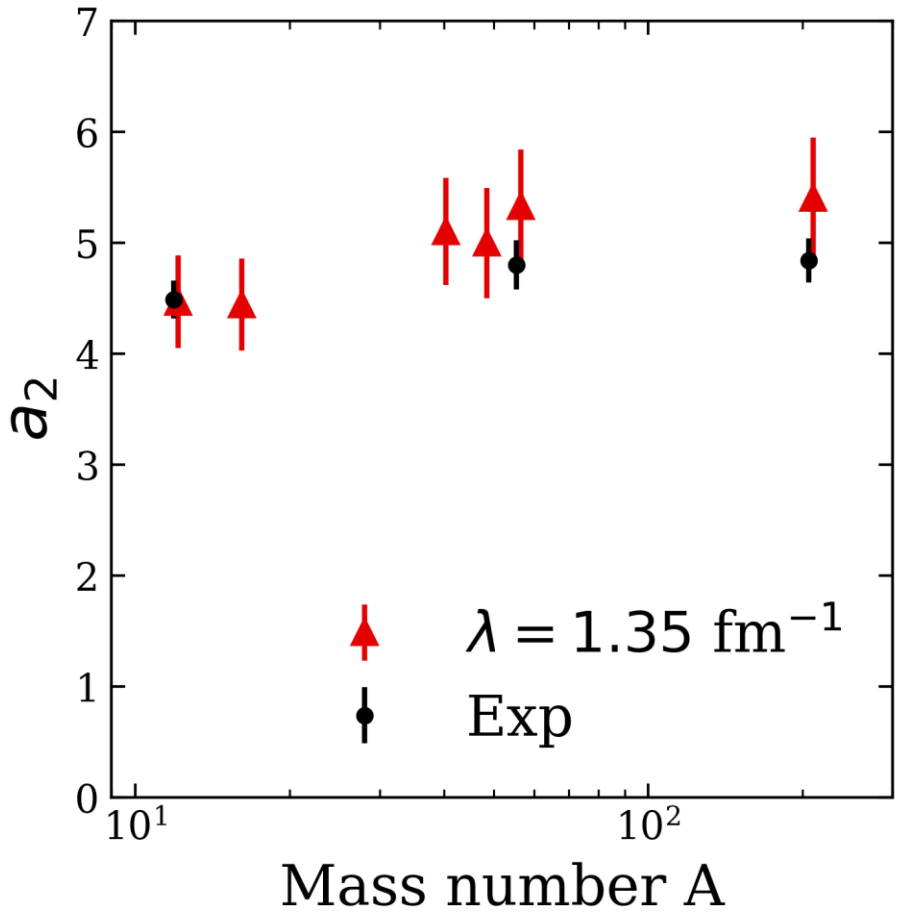

Fig. 10: a_2 scale factors using single-nucleon momentum distributions under LDA with AV18 and λ = 1.35 fm^{-1} compared to experimental values[1].

- SRC scale factors

$$a_2 = \lim_{q\to\infty} \frac{P^A(q)}{P^d(q)} \approx \frac{\int_{\Delta p^{high}} dq P^A(q)}{\int_{\Delta p^{high}} dq P^d(q)}$$

where $P^A(q)$ is the single-nucleon probability distribution in nucleus A

- Decent agreement with experiment[1] and LCA calculations[2] but need to further test systematics

[1]B. Schmookler et al. (CLAS), Nature **566**, 354 (2019)
[2]J. Ryckebusch et al., Phys. Rev. C **100**, 054620 (2019)

Summary and outlook

- Simple approximations work and are systematically improvable at low RG resolution
- Results suggest that we can analyze high-energy nuclear reactions using low RG resolution structure (e.g., shell model) and consistently evolved operators
  - Matching resolution scale between structure and reactions is crucial!
- Ongoing work:
  - Extend to cross sections and test scale/scheme dependence of extracted properties
  - Further investigate how final state interactions and physical interpretations depend on the RG scale
  - Apply to more complicated knock-out reactions (SRG with optical potentials) – see Mostofa Hisham’s talk (X13.00004)